Electric field and potential around localized scatterers in thin metal films studied by scanning tunneling potentiometry

Geetha Ramaswamy*

Department of Physics, Indian Institute of Science, Bangalore 560 012, India

A. K. Raychaudhuri†

National Physical Laboratory, New Delhi 110 012, India.

Abstract

Direct observation of electric potential and field variation near local scatterers like grain boundaries, triple points and voids in thin platinum films studied by scanning tunneling potentiometry is presented. The field is highest at a void, followed by a triple point and a grain boundary. The local field near a void can even be four orders of magnitude higher than the macroscopic field. This indicates that the void is the most likely place for an electromigration induced failure. The field build up near a scatterer strongly depends on the grain connectivity which is quantified by the average grain boundary reflection coefficient, estimated from the resistivity.

*email: geetha@physics.iisc.ernet.in

†email: arup@csnpl.ren.nic.in

Electromigraion (EM) failure is an important reliability issue for metallic interconnects in integrated circuits. Increased device density has caused a reduction in interconnect size, resulting in very high current densities which in turn increase the probability of EM failure. EM failures occur either by voids developing across the interconnects producing an open circuit or by extrusions which cause a short circuit with neighbouring lines. Due to its technological importance, the mechanism of field induced void formation has been studied by various techniques including microscopy based techniques[1,2]. Bamboo lines have a nanostructure consisting of a number of grain boundaries (GB) spanning the length of the interconnect. Near bamboo lines contain triple points (TP) and voids (V) along with a network of GBs. The electric field across such a thin film is not uniform at the nanometric scale and inhomogeneities in the field and current density occur near these localized scatterers[3]. The technique of scanning tunneling potentiometry (STP) invented by Muralt and Pohl[4], which is built around a scanning tunneling microscope (STM), offers a novel method of studying the potential variations and hence the electric field at these scattering centers with a nanometric resolution, by providing a simultaneous map of the topograpy and the potential distribution in a current carrying film. Thus it provides information regarding the nanostructure and the field distribution, both of which are of vital importance in EM studies.

In this letter we present our results on the study of electronic transport in polycrystalline thin platinum films by STM/STP. By simultaneously mapping out the topography and the potential distribution in the current carrying thin film, we investigate the variation in the potential and the build up of an electric field near various types of localized scatterers, in the scale of the spatial extent of the scatterers. We show that the spatial distribution and the magnitude of the local field depends on the type of the scatterer as well as the connectivity of the grains. Specifically, our experiments show that of the different types of scatterers present in a polycrystalline thin film, the maximum build up of an electric field occurs near a void, which then is the most likely spot for an EM induced failure. Further our study also shows that for a given type of scatterer, the magnitude of the local field depends on the grain connectivity and it is low for well connected grains.

Previous STP studies on metallic films have focused on charging effects in granular gold films[4] and on local variations in potential in Au-Pd[5], Au[6] and Bi thin films[7]. However, local variations in electric field around various kinds of extended defects occurring in a thin film has, so far, not been studied. Ideally, the STP experiments should be performed on conventional interconnect materials like Al and Cu. However, the formation of surface oxides in these materials on exposure to ambient atmosphere makes the interpretation of STP results difficult. In an attempt to understand the microscopic origin of the field inhomogeneities and the relative importance of the different kinds of defects in inducing an EM failure, we decided to study the underlying physical process in platinum, which is resistant to oxidation.

Platinum films (thickness$\approx$10 nm, deposition rate $\approx$2.8 nm/min) were deposited using shadow masks on cleaned glass substrates by e-beam in a turbo pumped chamber at a base pressure of 5 X 10^{-8} torr, using material of 6N purity. Simultaneous STM/STP images were obtained by the double feedback technique, imaging the films under ambient conditions in an STM built in-house, using Pt-Rh(13%) tips. The details of the STM and the double feedback operation have been described elsewhere[8,9]. The topographic images were obtained with a tunnel current of I_{pp} = 0.8 nA and an AC bias of V_{pp} = 0.05 V at a frequency of

2 kHz. The potentiometic images were obtained with a macroscopic field of 5.2 V/cm and a current density $\mathbf{j} \approx 10^5$ A/cm^2. To avoid any artifacts that might arise if the current direction and the scan direction are the same, $\mathbf{j}$ was kept at an angle (-70^o) to the fast scan direction (X axis).

Figure 1 (a) and (b) show the simultaneous STM and STP images respectively, in a 62 nm X 44 nm region of the film. The topographic image shows a number of grains, GB, TP and V. Representative ones are marked in the figure. The nanostructure consists mostly of circular grains having an average grain diameter $< D > \approx 14.7$ nm and an r.m.s surface roughness ≈ 1.6 nm, as obtained from several topographic scans performed in different regions of the film. Fig. 1(c) is a line profile across the topographic image (marked across the image) showing the z-height corrugations of the GBs and TPs. From the potentiometric image and the line profile shown in Fig. 1(d), it is immediately apparent that the potential does not drop uniformly across the film surface and that the local potential distribution is severely affected in the vicinity of the scatterers. The line profile in Fig. 1(d) is obtained across the potential image in the same region as the profile in Fig. 1(c). From the two line profiles we discern a one to one correspondence between the scattering centers in the topographic image and the voltage variations in the potential image.

We analysed the STP images obtained from various regions of the film to ascertain the magnitude of the potential inhomogeneities caused by different types of extended defects and their relative importance in contributing to a possible EM failure. Our analysis shows that the typical potential variations $\Delta\phi$ at the GB are $\approx$ 1 - 3 mV occurring over a range of 0.5 - 3.5 nm. At the TP and voids $\Delta\phi$ is $\approx$ 1 - 4 mV and 3 - 9 mV respectively, occurring over a distance of 1 - 3 nm. It is to be noted that the potential image is flat and featureless in the absence of a DC current through the sample, except for a few 0.3 mV quantization noise wiggles of the A/D converter, as seen from Fig. 1(e). This proves that the potential variations are the result of an actual build up of a field near the scatterer and are not due to tip related artifacts.

In order to further understand the nature of the grain connectivity and the extent and magnitude of the scattering at different scattering centers such as GB, TP and V, we investigated the electric field values in their vicinity. The local transport field in the surface plane is calculated from the gradient of the local potential, $\phi(x, y)$, as: $\mathbf{E}_{\|}(x, y) = - \nabla\phi(x, y)$. $\phi(x, y)$ is what is measured in an STP scan. We computed the electric fields along the X, Y directions numerically from the 128 X 128 potentiometric data array and used quiver plots of the field data to visually show the distribution of field lines near the scatterer. The results of the field calculation are shown in Fig. 2. The length of the arrow indicates the magnitude and the head points along the direction of the field.

Figure. 2 shows the electric field and a line scan across the potential image around a GB, a TP and a V. These regions have been labeled and marked by a rectangle in Fig. 1(a), with a short line across the rectangle depicting the profile. A comparison of the figures brings out the distinct nature of the electric field distribution around the three kinds of scatterers. The field lines in a GB (Fig. 2(a)) are concentrated along the periphery of the grain and very low in its interior. At a TP the field lines are stronger (Fig. 2(c)). The field radiates outward from the GB and concentrates at the TP. At a V, the build up of the field is most prominent (Fig. 2(e)). This is also brought out by the STP line profiles (Figs. 2(b),(d),(f)), which show that the potential inhomogeneity is a maximum at a V and minimum at a GB. Typical field

values obtained from above are $\approx$ 1.6 X 10^4 V/cm, 3.2 X 10^4 V/cm and 7.2 X 10^4 V/cm respectively for a GB, TP and V.

Our study also indicates that the field build up around a scatterer will depend on the grain connectivity for a given kind of scatterer. The grain connectivity of the film can be characterized by an average GB reflection coefficient ¡R$_g$¿, which is obtained from an analysis of the temperature dependence of resistivity of the film[10,11]. From the analysis of the resistivity data ($\rho_{4.2K}\approx 47\mu\Omega$cm and $\rho_{300K}/\rho_{4.2K}$=1.05), we obtain an ¡R$_g$¿$\approx$0.9 for this film. In order to better understand the dependence of ¡R_g¿ on the grain connectivity, which is reflected in the field build up, we repeated the STM/STP experiments on a platinum film which was grown on a rougher surface but with similar thickness and average nanostructural parameters ($< D >\approx$12.35 nm and an r.m.s roughness of 1.7nm). The film had a $\rho_{4.2K}\approx 160\mu\Omega$cm and $\rho_{300K}/\rho_{4.2K}$=1.22, resulting in a ¡R_g¿$\approx$0.97. This shows that the grains are not as well connected as in the previous film. In this film, although the STP and the field patterns are qualitatively similar to the previous film, for the same macroscopic field, the magnitude of the field at the defects (GB, TP and V) are an order of magnitude larger. This clearly indicates that the field build up, for a particular kind of defect, strongly depends on the grain connectivity.

This study has brought out a number of important observations. The quiver plots conclusively prove that the field across the film is not uniform and it is severely altered at the scatterers. Further, the field tends to concentrate at the scatterer and it is very low in the interior of the grain. The magnitude of the field, for a given scatterer, depends on the grain connectivity. Among the different kinds of scatterers, the field is highest at a void. The mapping out of the potential and field at the different scattering sites is an important result as this has significant implications on our understanding of EM phenomena in an interconnect. It identifies regions of excessive field build up, which are the likely "weak spots" where an EM failure can originate. Previous studies on thin films have shown that during EM, vacancies migrate predominantly along GBs and accumulate at GBTPs due to vacancy flux divergence[12,13]. These vacancies coalesce into a void, which then becomes the most likely spot for an EM failure to occur, when it reaches a critical size. Our STP study supports this observation. If the grain connectivity is poor, the local field at a triple point may even be three orders of magnitude higher than the average macroscopic value. Such a high field can result in a void formation, which has a higher field build up and hence has the greatest probability for EM induced film failure.

In conclusion, we have established a procedure for identifying the hot spots for a field induced EM failure. Our study shows that wide line metal interconnects should have well connected grains with a minimum number of triple points and voids for reliable long term performance.

We wish to thank Prof. N. Chandrasekhar for allowing us the use of his e-beam facility and K. Das Gupta for depositing the films.

REFERENCES

[1] E. Arzt, O. Kraft, W. D. Nix, and J. E. Sanchez Jr., J. Appl. Phys. **76**, 1563 (1994).
[2] P. Besser, M. C. Madden, and P. A. Flinn, J. Appl. Phys **72**, 3792 (1992).
[3] R. Landauer, IBM J. Res. Dev. **1**, 223 (1957).
[4] P. Muralt and D. W. Pohl, Appl. Phys. Lett. **48**, 514 (1986).
[5] J. R. Kirtley, S. Washburn, and M. J. Brady, Phys. Rev. Lett. **60**, 1546 (1988).
[6] M. A. Schneider, M. Wenderoth, A. J. Heinrich, M. A. Rosentreter, and R. G. Ulbrich, Appl. Phys. Lett. **69**, 1327 (1996).
[7] B. G. Briner, R. M. Feenstra, T. P. Chin, and J. M. Woodall, Phys. Rev. B **54**, R5283 (1996).
[8] Geetha Ramaswamy, A. K. Raychaudhuri, K. Das Gupta, and G. Sambandamurthy, Appl. Phys. A **66**, S435 (1998).
[9] Geetha Ramaswamy, Ph.D Thesis, Indian Institute of Science, Bangalore, India, May 1998.
[10] J.R. Sambles, Thin Solid Films **106**, 321 (1983).
[11] Geetha Ramaswamy, A. K. Raychaudhuri, J. Goswami, and S. A. Shivashankar, J. Appl. Phys. **82**, 3797 (1997).
[12] M. J. Attardo and R. Rosenberg, J. Appl. Phys. **41**, 2381 (1970).
[13] P. S. Ho and T. Kwok, Rep. Prog. Phys. **52**, 301 (1989) and references therein.

FIGURE CAPTIONS

(1) FIG.1. Simultaneous STM/STP scans in a 62 nm X 44 nm area. (a) topographic scan (b) potentiometric scan. The arrow indicates the direction of the macroscopic **j**. The profiles across (a) and (b) are shown in (c) and (d) respectively. (e) STP profile in the absence of a field.

(2) FIG. 2. The field distributions and line profiles at various types of scatterers, calculated from the STP image, obtained in the regions marked by rectangles and short lines respectively in Fig. 1(a). (a) and (b) Field and profile at a GB, (c) and (d) at a TP and (e) and (f) at a V. It is seen that the field is maximum at a void, followed by a TP and a GB and it is very low in the interior of the grain.

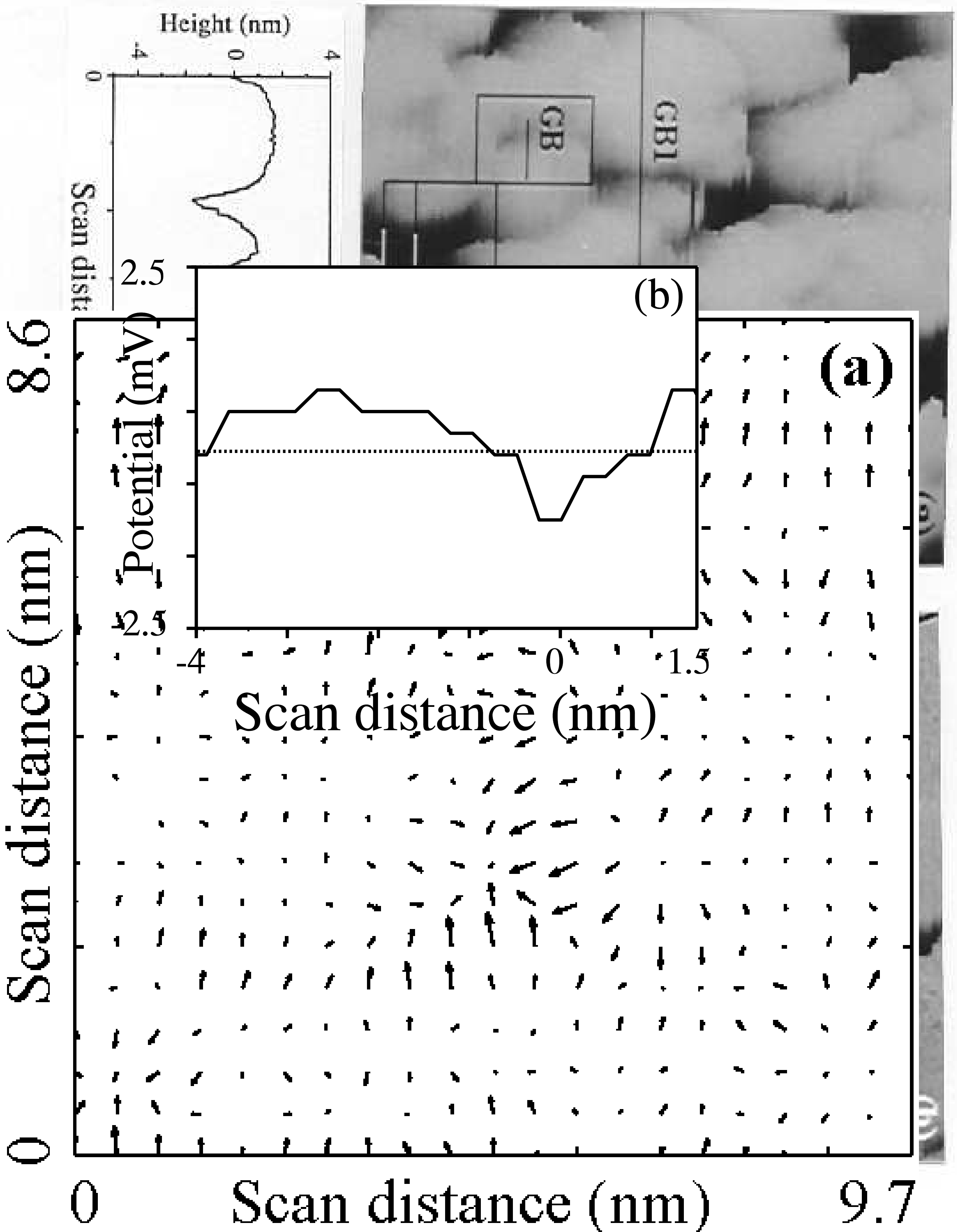
Height (nm)
4
0
4
0
GB
GB1
(b)
2.5
-2.5
Potential (mV)
-4
0
1.5
Scan distance (nm)
(a)
8.6
0
Scan distance (nm)
0
9.7
Scan distance (nm)

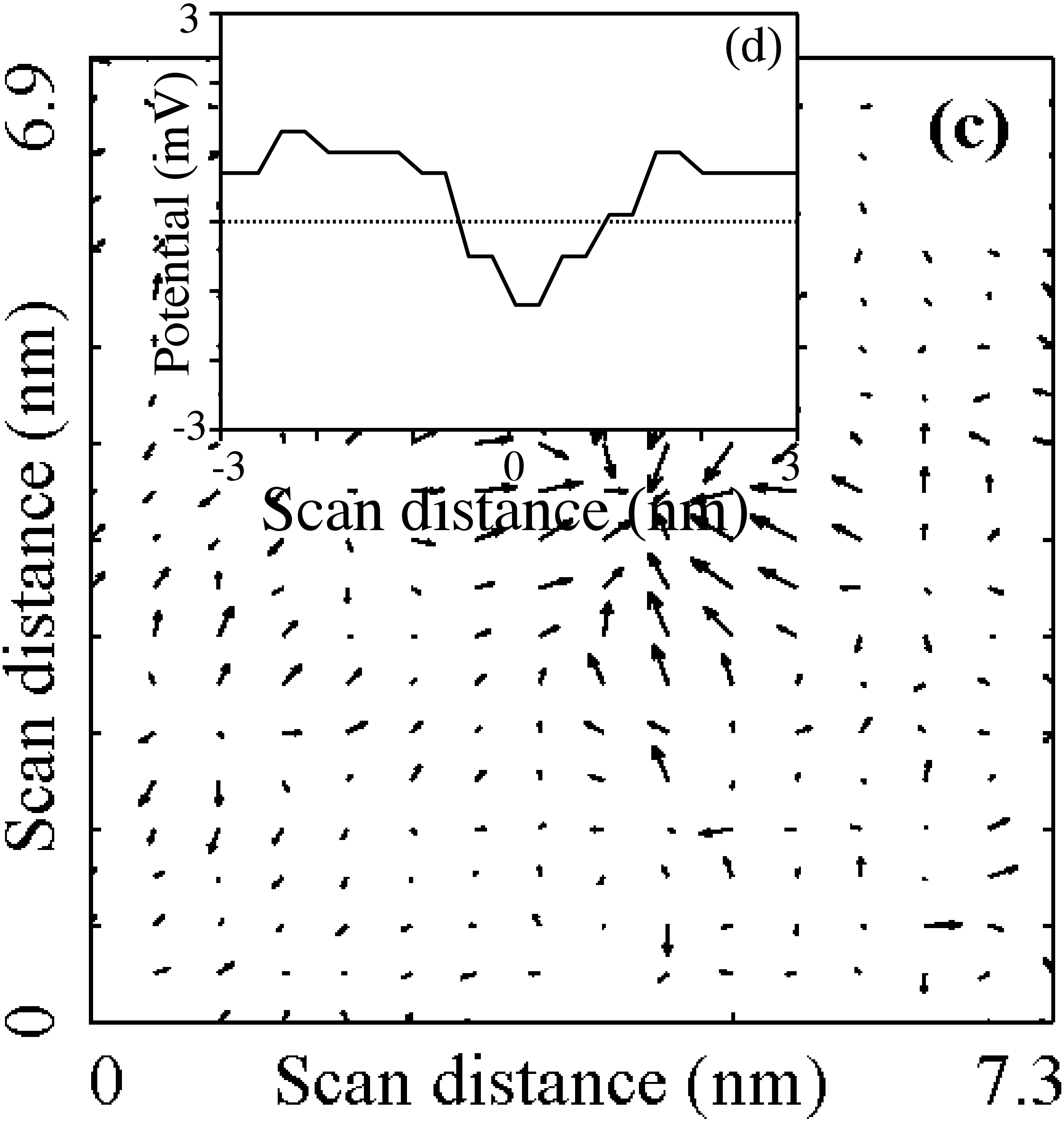
3
(d)
Potential (mV)
-3
-3
0
3
Scan distance (nm)
(c)
6.9
Scan distance (nm)
0
0
Scan distance (nm)
7.3

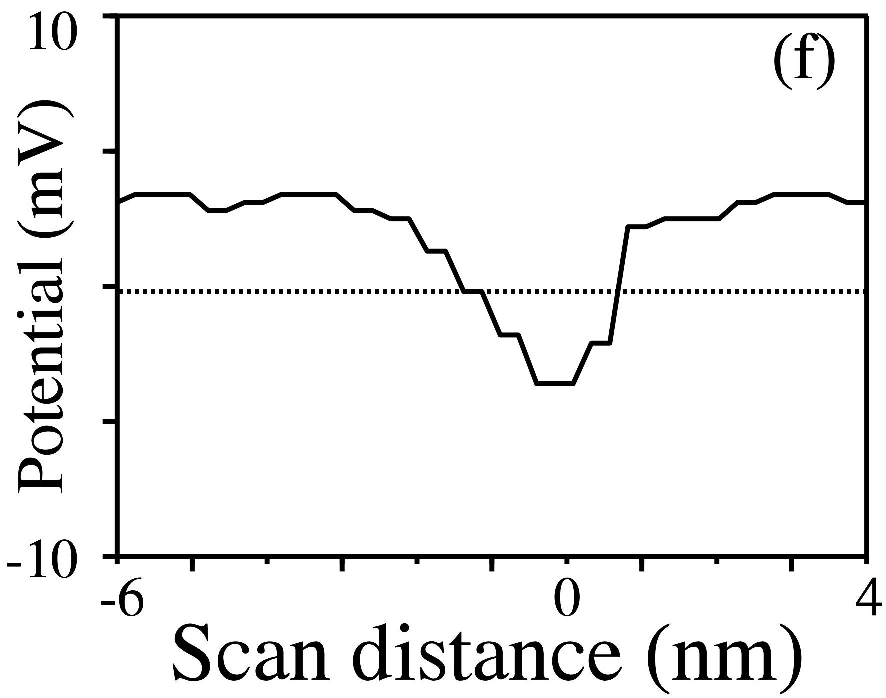
10
(f)
Potential (mV)
-10
-6
0
4
Scan distance (nm)